

PERFORMANCE CHARACTERISTICS OF AN MHD
PILOT PLANT ELECTROSTATIC PRECIPITATOR

J. S. Lindner, P. R. Jang, W. P. Okhuysen
Diagnostic Instrumentation and Analysis Laboratory
Mississippi State University
Mississippi State, MS 39762

and
J. K. Holt
Energy Conversion Program
University of Tennessee Space Institute
Tullahoma, TN 37388

Keywords: Magnetohydrodynamics, ESP, Real-time diagnostics

INTRODUCTION

In magnetohydrodynamic (MHD) power generation a seed material, normally K_2CO_3 , is added to enhance the conductivity of the coal-fired gas stream. The plasma is passed through a magnetic field and electricity is produced by the Hall effect. Future large scale MHD facilities are expected to be more efficient than conventional coal-fired power plants not only because of the DC electricity produced but also from increased heat recovery owing to the large (3000 K) combustion temperatures employed.

There is, however, a finite cost for the seed material and the resulting K_2SO_4 particles (SO_2 emissions are minimized by combination with seed potassium) must be collected, converted back to K_2CO_3 or KCO_2H , and recycled back to the combustor. Although estimates vary it is well recognized that a large portion ($\geq 95\%$) of the spent seed must be recycled for viable economic operation.¹

The performance characteristics of the MHD electrostatic precipitator (ESP) are therefore of interest. As an added condition recent experimental and theoretical studies of K_2SO_4 homogeneous nucleation² have indicated that these particles grow to Sauter diameters of between 1 and 1.2 μm . These sizes are in a range where ESP performance may be degraded.³

In this work, we describe Mie scattering and electric field measurements on an MHD pilot scale ESP located at the Coal Fire Flow Facility (CFFF) at the University of Tennessee Space Institute. Results are reported for the determination of near-real-time collection efficiencies, the variation of the ESP performance with seed percentage, and initial studies on the extent of particle re-entrainment.

EXPERIMENTAL

The theoretical framework for determination of the Sauter mean diameter, D_{32} , using two-color laser transmissometry has been reported previously.^{4,5} Briefly, transmissions ($T = I/I_0$) measured at two well-separated monochromatic wavelengths (λ_1, λ_2) are related to an extinction efficiency ratio which is proportional to D_{32}

$$\frac{\ln T(\lambda_2)}{\ln T(\lambda_1)} = \frac{\bar{Q}_2}{\bar{Q}_1} D_{32} \quad (1)$$

Mie theory is used to calculate the variation of \bar{Q}_2/\bar{Q}_1 , (bars indicate averages over a distribution) on D_{32} . For the case of a polydisperse particle size distribution (PSD) \bar{Q} is expressed in terms of an effective extinction cross section, $\bar{\sigma}$, and an assumed distribution

$$\bar{Q} = \int_0^{\infty} \bar{\sigma}_a f_N(r) dr / \pi \int_0^{\infty} r^2 f_N(r) dr \quad (2)$$

where $\bar{\sigma}_a$ is calculated from the theory with knowledge of the complex refractive index, m .

The theoretical response curve used to interpolate D_{32} from the measured transmissions (insert Figure-1) is generated by scaling the assumed PSD. Each distribution corresponds to a unique D_{32} value. The effect of the PSD shape on D_{32} has been determined by sensitivity studies⁶ to be within -2% or +9% of the integrated D_{32} value. This result is consistent with the fact that D_{32} is, by definition, a z-average quantity.

Studies have also been carried out on the effect of the complex refractive index on D_{32} ⁶. Using the reported values⁴ of m for Illinois #6 and Montana Rosebud with and without spent seed (K_2SO_4) and the m value for K_2SO_4 it was determined the D_{32} varies by $\pm 0.1 \mu m$. The above result has some implications on the work reported here as the chemical composition of the particles⁷ entering the CFFF ESP are about 85% K_2SO_4 with the remainder flyash. Thus the use of the complex refractive index for K_2SO_4 is not expected to have a significant effect on the Sauter diameters determined.

Although the primary observable in two-color extinction measurements is D_{32} additional information concerning mass and number loading can be obtained. Number densities, C_n values, are available from Beer's law

$$T(\lambda) = \exp(-l\bar{\sigma}_\lambda C_n) \quad (3)$$

where l is the effective optical path length. The mass density C_m is related to C_n through the chemical density, d , of the particles and the volume density, C_v

$$C_m = dC_v = (d4\pi r_{32}^3 C_n) / 3 \quad (4)$$

Electron micrographs of particles collected downstream of the CFFF superheater indicate spherical shape.⁷

The optical configuration of one of the two-color laser transmissometer (TCLT) units is shown in Figure 1. The second optical unit is similar to that shown with the exception that only two lasers, an argon ion ($\lambda = 0.488$ or $0.5145 \mu m$) and a helium-neon ($\lambda = 3.39 \mu m$) are used. For the efficiency measurements both units were interfaced to the microprocessor unit. Because of a small but finite time delay of 100 ms (the processor collects raw intensities from one optical unit followed by the intensities from the second unit) the measurements reported here are classified as nearly simultaneous. For the experiments on rapid temporal response the microprocessor unit was replaced by an IBM PC/AT type microcomputer with an analog to digital board.

Electric field meter (EFM) measurements were performed using a laboratory built unit similar to that reported by Castle et al.⁸ The field was sensed by four circular electrodes whose signals were modulated using a 4-hole chopper wheel powered by an air motor. Laboratory experiments indicated that the output of the meter was constant to within ± 1 mv over the frequency range from 220 to 270 hr. Initially the meter was calibrated⁹ using parallel plates where

$$E = V/D \quad (5)$$

Here E is the electric field, V the applied plate voltage and D the distance between the meter and the charged plate. Knowledge of the duct geometry permits the solution of Poisson's equation for the space charge density, ρ . Expressions for E in terms of ρ for cylindrical⁸ and rectangular¹⁰ ducts have been reported. Calculations for the trapezoidal exit duct of the CFFF ESP have not yet been performed; consequently, only raw voltages are reported here. These data are, however, directly related to ρ which is usually expressed in C/m³ units. Each particle exiting the ESP will carry some charge, q, thus ρ/q yields a measure of number concentration. Results from the EFM are then comparable to the scattering method but also provide the charge density which is an important parameter in models of electrostatic precipitation.¹¹

Location of the TCLT units and the EFM with respect to the CFFF ESP is given in Figure - 2. Experiments reported here correspond to facility tests LMF4-N, LMF4-S and LMF4-U. Near-real-time collection efficiencies determined during LMF4-N were calculated from the penetration, P

$$P = \left(\frac{Cn(out)}{fCn(in)} \right) (100) \quad (6a)$$

$$Efficiency = 100 - P \quad (6b)$$

in the above equation f is that fraction of the total flow diverted to the ESP. The values of f were taken from the CFFF records where information on the electrical conditions of the ESP, temperatures, vibrator and plate-rapping frequencies and other pertinent conditions are collected.

RESULTS AND DISCUSSION

As stated previously, the behavior of the MHD ESP is critical to the successful economic operation of the facility. The three studies below represent only a fraction of the results collected to date. The data on efficiency and the performance of the ESP as a function of the ratio K_2/S have practical bearing on future commercial scale facilities. The final study concerns our initial efforts to characterize rapid temporal variations of ESP performance and the application of the field meter.

Near - Real - Time Efficiency Measurements - Average Sauter diameters determined upstream of the ESP are collected in Figure - 3. An average of $1.2 \mu m$ was calculated. Measurements on May 6 and 7 yielded D_{32} values of 1.18 and $1.25 \mu m$ respectively. Average number densities were $5.6, 4.8$ and $4.2 \times 10^6 \text{ cm}^{-3}$.

Extinction measurements downstream of the ESP permit the application of Eq. 6. Corresponding efficiency values are presented in Figure - 4. To our knowledge this data represents the first reported determination of near - real - time efficiencies for an electrostatic precipitator. In this regard it should be noted that the application of standard sample extraction methods can only provide an estimate of the efficiency since the sampling times before and downstream of the ESP will not be the same. Additionally, any changes in facility operation cannot be quantified rapidly.

Although some scatter is observed in Fig. 4 the majority of efficiencies lie above 90% with many values larger than 95%. The radical decrease in efficiency between 1348 and 1408 hours corresponds to a baghouse cleaning cycle. During this process the flow normally partitioned to the fabric filter device was diverted to the ESP, thereby increasing the flow by approximately 5000 cfm. The decrease in efficiency, albeit of short duration, indicates that the ESP cannot completely

adjusted to the additional mass loading. This result is expected based on the flow entering the device, 16,400 cfm compared to the design set point of about 8600 cfm.¹²

Some comments are required concerning the factor f appearing in Eqs. 6. Using C_N values of 2.5×10^5 (outlet) and $5.98 \times 10^6 \text{ cm}^{-3}$ (inlet) it is possible to determine the effect of errors in the mass flow on the efficiency. For the data in Fig. 4 (excluding the cleaning cycle) the flow to the ESP was measured as 11,000 cfm. The flow to the baghouse was 5400 cfm and the calculated efficiency was 94.3%. Assuming flows to the ESP of 9000 and 13,000 cfm yielded efficiencies ranging from 93 - 95.2% or a difference of slightly larger than 2%. So long as the flow rate to the ESP is known to within 20% the calculation of the efficiency is adequate.

Effect of the Ratio K_2/S - Initially feed rates to the MHD combustor were controlled to provide sufficient K atoms for plasma enhancement and the total conversion of SO_2 to K_2SO_4 . Recently it has been noted that generator power levels could be increased by overseeding.¹³ This practice led to variations in the performance of downstream components as noted by increased bridging in the platen superheater and decreased ESP performance¹⁴ presumably due to K_2CO_3 or other K species.

Measurements of the particle size and loading downstream of the CFFF ESP were conducted at different K_2/S (molar ratio of K in seed to S in coal) ratios during facility test LMF4-S. Figure - 5 illustrates Sauter diameters for time periods corresponding to different K_2/S ratios. Clearly, as the K_2CO_3 percentage decreases the D_{32} values increase.

During these measurements the facility conditions such as gas stream temperatures, soot blowing frequency, total coal flow and combustion stoichiometry, etc. were reasonably constant. The mass flow rates to the ESP were approximately 6000 cfm for the data in panels A and B and 7800 cfm in panel C. The previous efficiency results indicate that as the mass loading is increased (i.e. fabric filter cleaning cycles) the efficiency decreases. This corresponds to an increase in C_N (or a decrease in D_{32} , Eqs. 1 and 3) at the downstream location. The fact that D_{32} is increased at the K_2/S ratio of 1.04 (Fig. 5 panel C) indicates that the excess K_2CO_3 (panels A and B) has a significant effect on ESP performance.

The decreased ESP performance at large K_2/S ratios may indicate that the K_2CO_3 particles are nucleating to smaller particle diameters than K_2SO_4 . Changes in particle resistivity do not appear to be responsible for the observed behavior. Further studies are in progress.

Initial Studies of ESP Temporal Performance - The standard means of characterizing ESP operation involves the extraction of sample, preferably isokinetically, from the gas stream. The extraction requires some time and, thus, events occurring over periods of seconds or even minutes cannot be quantified. Such events are thought to be those due to collection plate rapping and the vibration of the wire racks. Experiments were initiated to evaluate the extent of particle re-entrainment from the CFFF ESP.

For these experiments conducted during test LMF4-U the electric field meter (EFM) was installed at the exit duct of the ESP and the TCLT was located slightly downstream. The K_2/S ratio was held constant at 1.0. Figure 6 illustrates the average Sauter diameters (top trace) and the raw EFM signal (lower trace) over a typical collection period. The average particle size is similar to that observed in panel C of Fig. - 5. Of interest in Fig. 6 is the increase in field meter voltage and the decrease in D_{32} observed at approximately 1217. The locations of the peaks are shifted relative to one another owing to the fact that the computer clocks were not synchronized (the residence time between the instrument locations has been calculated at 1 sec.).

Examination of the facility data records led to the assignment of the increase in C_N to the vibration of the field 4 wire rack. Although there could be similar information on the effects of the vibrators for fields 1, 2 and 3 as well as on plate rapping the noise in the data precludes unequivocal assignment. The apparent lack of particle re-entrainment from rapping may arise from the 2 min. frequency for this process. Further studies wherein the frequency of rapping and wire rack vibrating are varied are in progress.

CONCLUSIONS

Our studies of the CFFF pilot plant ESP have yielded some valuable information concerning the performance of the component under different MHD facility operating conditions. To our knowledge, this is the first report of the determination of ESP efficiency in near-real-time. Studies on the ratio K_2/S indicate that ESP performance degrades as the ratio is increased. Work is in progress to further quantify this effect and to establish the conditions for efficient ESP operation at overseeding conditions. Initial temporal studies conducted downstream of the ESP indicate that particle re-entrainment from vibration of the wire racks is more pronounced than increased emission from collection plate rapping.

ACKNOWLEDGEMENTS

We acknowledge support of this work through DOE contract DE-AC01-80ET-15601 to the Diagnostic Instrumentation and Analysis Laboratory at Mississippi State University and DOE contract DE-AC02-79ET-10815 to the Energy Conversion Program at the University of Tennessee Space Institute.

REFERENCES

1. Petrick, M.; et al., in Open Cycle Magnetohydrodynamic Electrical Power Generation, M. Petrick and B. Ya Shumyatsky, eds. Argonne National Laboratory, Argonne, IL (1978).
2. Wang, C. and Lindner, J. S., *J. Prop. Pow.* **6**, 552 (1990).
3. ASHRAE Handbook - Equipment, American Society of Heating, Refrigerating and Air Conditioning Engineers Atlanta, GA (1988).
4. Ariessohn, P. C., HTGL Report No. 119, Stanford University, Stanford CA (1980).
5. Dobbins, R. A. and Jizmagian, G. S., *J. Opt. Soc. Am.* **56**, 10 (1966).
6. Lindner, J. S.; et al., Proceedings of the 27th Symposium on the Engineering Aspects of Magnetohydrodynamics p. 8.5.1 Reno NV. (1988)
7. Holt, J. K. et al., Proceedings of the 25th Symposium on the Engineering Aspects of Magnetohydrodynamics p. 8.2.1, Bethesda, MD (1986).
8. Castle, G. S. P.; et al. *IEEE Trans. Ind. Appl.* **24**, 702 (1988).
9. Blitshteyn, M. *Eval. Eng.* p. 70 Nov. (1984).
10. Carruthers, J. A. and Wigley, K. J., *J. Inst. Pet.* **48**, 180 (1962).
11. Lawless, P. A. and Sparks, L. E., *IEEE Trans. Ind. Appl.* **24**, 922 (1988).
12. Morehead, B. K. and Foote, J. P., Proceedings of the 23rd Symposium on the Engineering Aspects of Magnetohydrodynamics p. 585 Somerset, PA (1984).
13. Stepan, I. E.; et al., Proceedings of the 28th Symposium on the Engineering Aspects of Magnetohydrodynamics p. 1.1-1, Chicago IL (1990).
14. Attig, R. C.; et al., Proceedings of the 27th Symposium on the Engineering Aspects of Magnetohydrodynamics p. 1.2-1 Reno NV (1989).

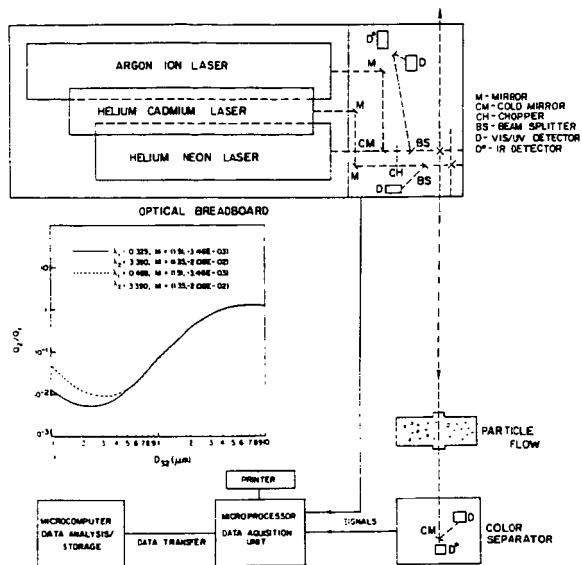


Figure 1. Experimental configuration and theoretical response curve for the Two-Color Laser Transmissometer.

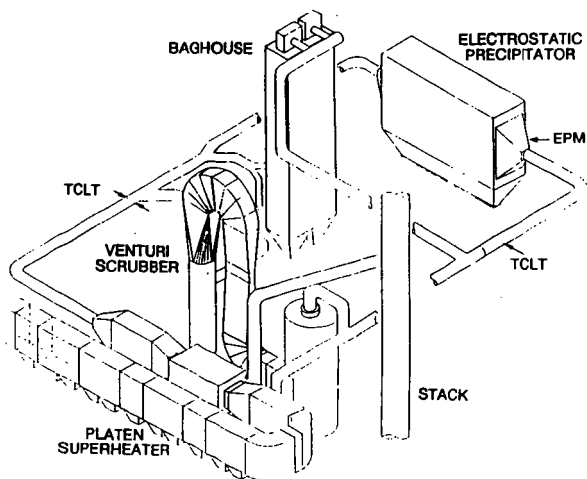


Figure 2. Instrument locations with respect to the downstream facility components of the Coal-Fired Flow Facility.

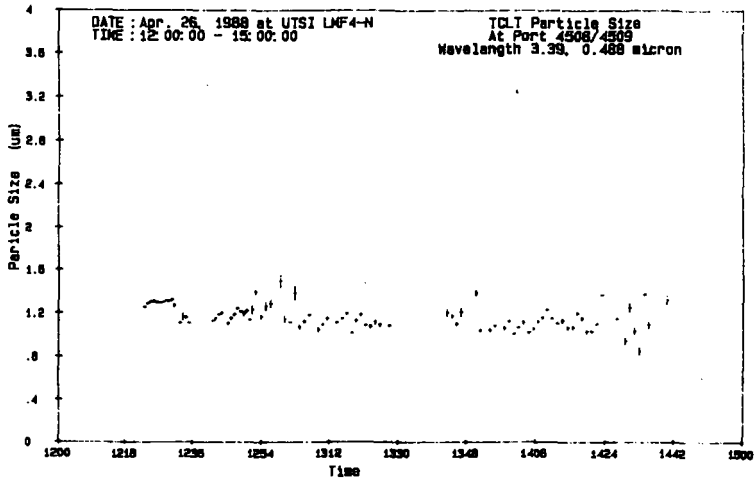


Figure 3. Average particle sizes (D_{32} values) at the baghouse/ESP inlet.

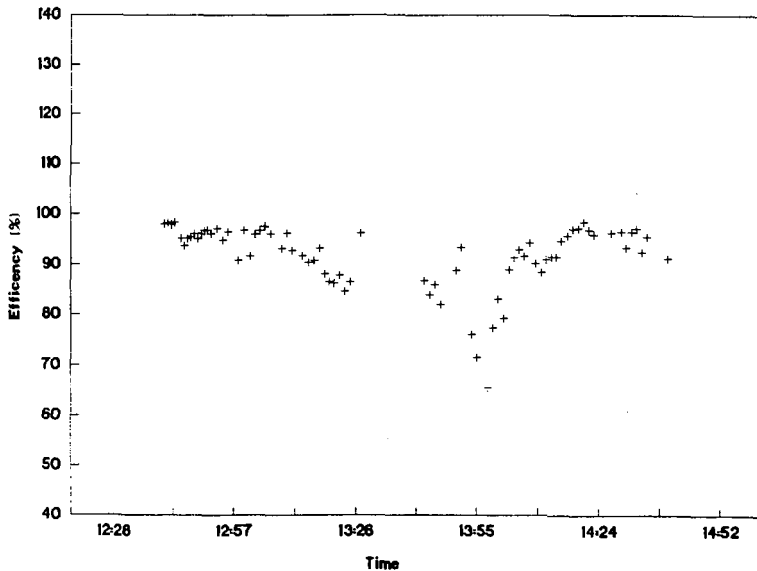


Figure 4. Near-real-time ESP efficiencies measured during LMF4-N. The decrease in efficiency around 1355 corresponds to a baghouse cleaning cycle with all flow diverted to the ESP.

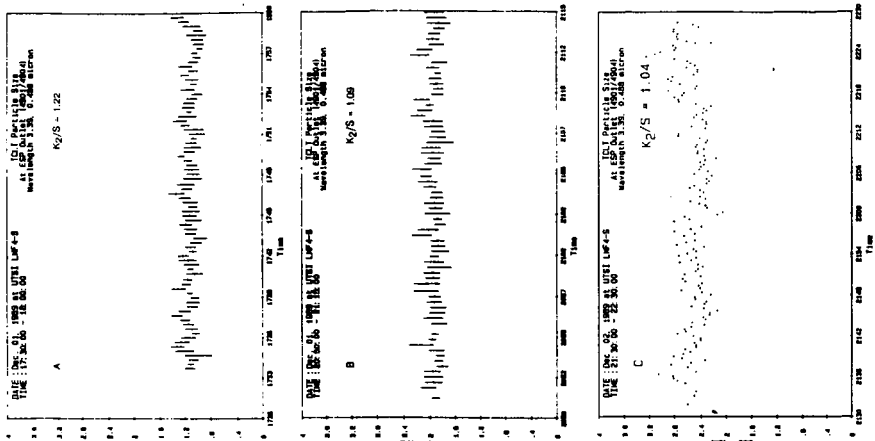


Figure 5. Average Sauter diameters measured at the outlet of the ESP during facility test LMF4-S. Values of the ratio K_2/S decrease in going from panel A to panel C.

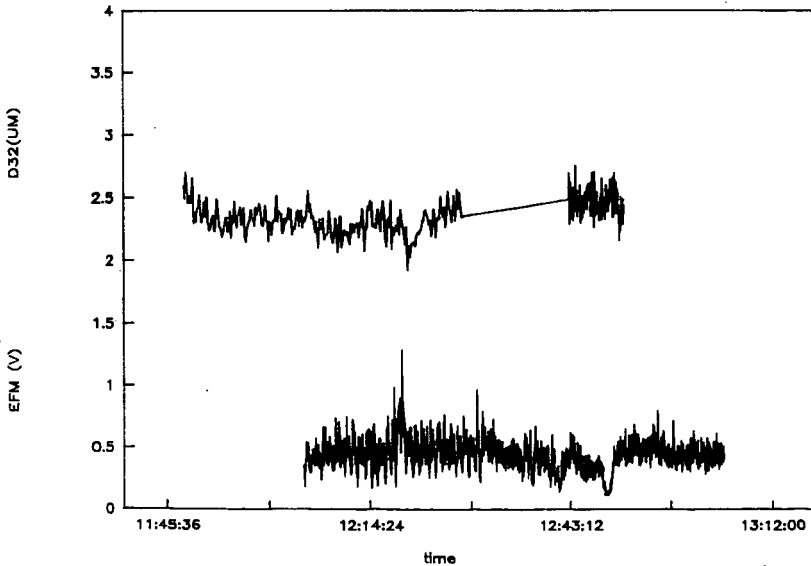


Figure 6. Average Sauter diameter (top trace) and EFM voltage measured during facility test LMF4-U. The decrease in D_{32} and increase in EFM voltage corresponds to particle re-entrainment originating from vibration of the field 4 wire racks.